BRAIN COMMUNICATIONS

Intraoperative microseizure detection using a high-density micro-electrocorticography electrode array

James Sun,[1,*] Katrina Barth,[2,*] Shaoyu Qiao,[1] Chia-Han Chiang,[2] Charles Wang,[2] Shervin Rahimpour,[3,4] Michael Trumpis,[2] Suseendrakumar Duraivel,[2] Agrita Dubey,[1] Katie E. Wingel,[1] Iakov Rachinskiy,[2] Alex E. Voinas,[1] Breonna Ferrentino,[1] Derek G. Southwell,[3,5] Michael M. Haglund,[3] Allan H. Friedman,[3] Shivanand P. Lad,[3] Werner K. Doyle,[6] Florian Solzbacher,[7,8,9] Gregory Cogan,[3,10,11,12,13] Saurabh R. Sinha,[12,13] Sasha Devore,[14] Orrin Devinsky,[6,14,15] Daniel Friedman,[14] Bijan Pesaran[1,14] and Jonathan Viventi[2,3,5,12]

* These authors contributed equally to this work.

One-third of epilepsy patients suffer from medication-resistant seizures. While surgery to remove epileptogenic tissue helps some patients, 30–70% of patients continue to experience seizures following resection. Surgical outcomes may be improved with more accurate localization of epileptogenic tissue. We have previously developed novel thin-film, subdural electrode arrays with hundreds of microelectrodes over a 100–1000 mm^2 area to enable high-resolution mapping of neural activity. Here, we used these high-density arrays to study microscale properties of human epileptiform activity. We performed intraoperative micro-electrocorticographic recordings in nine patients with epilepsy. In addition, we recorded from four patients with movement disorders undergoing deep brain stimulator implantation as non-epileptic controls. A board-certified epileptologist identified microseizures, which resembled electrographic seizures normally observed with clinical macroelectrodes. Recordings in epileptic patients had a significantly higher microseizure rate (2.01 events/min) than recordings in non-epileptic subjects (0.01 events/min; permutation test, $P = 0.0068$). Using spatial averaging to simulate recordings from larger electrode contacts, we found that the number of detected microseizures decreased rapidly with increasing contact diameter and decreasing contact density. In cases in which microseizures were spatially distributed across multiple channels, the approximate onset region was identified. Our results suggest that micro-electrocorticographic electrode arrays with a high density of contacts and large coverage are essential for capturing microseizures in epilepsy patients and may be beneficial for localizing epileptogenic tissue to plan surgery or target brain stimulation.

1 Center for Neural Science, New York University, New York, NY, USA
2 Department of Biomedical Engineering, Duke University, Durham, NC, USA
3 Department of Neurosurgery, Duke University School of Medicine, Durham, NC, USA
4 Department of Neurosurgery, Clinical Neuroscience Center, University of Utah, Salt Lake City, UT, USA
5 Department of Neurobiology, Duke University School of Medicine, Durham, NC, USA
6 Department of Neurosurgery, NYU Grossman School of Medicine, New York, NY, USA
7 Department of Electrical and Computer Engineering, University of Utah, Salt Lake City, UT, USA
8 Department of Biomedical Engineering, University of Utah, Salt Lake City, UT, USA
9 Department of Materials Science & Engineering, University of Utah, Salt Lake City, UT, USA
10 Department of Psychology and Neuroscience, Duke University, Durham, NC, USA
11 Center for Cognitive Neuroscience, Duke University, Durham, NC, USA

Received October 05, 2021. Revised February 10, 2022. Accepted May 24, 2022. Advance access publication May 27, 2022

12 Duke Comprehensive Epilepsy Center, Duke University School of Medicine, Durham, NC, USA
13 Department of Neurology, Duke University School of Medicine, Durham, NC, USA
14 Department of Neurology, NYU Grossman School of Medicine, New York, NY, USA
15 Department of Psychiatry, NYU Grossman School of Medicine, New York, NY, USA

Correspondence to: Jonathan Viventi 1149 CIEMAS, 101 Science Dr Durham, NC, 27705, USA E-mail: j.viventi@duke.edu

Correspondence may also be addressed to: Bijan Pesaran 4 Washington Pl, New York NY, 10003, USA E-mail: bijan@nyu.edu

Keywords: epilepsy; microseizure; ECoG; intraoperative; microelectrode

Abbreviations: DBS = deep brain stimulation; ECoG = electrocorticography; EZ = epileptogenic zone; kSPS = kilo samples per second; LCP = liquid crystal polymer; LCP-TF = liquid crystal polymer thin-film; LFP = local field potential; LL = line length PtIr = platinum–iridium; RNS = responsive neurostimulation; sEEG = stereo-electroencephalography; TF = thin film; μECoG = micro-electrocorticography; μHDMI = micro high-definition multimedia interface

Graphical Abstract

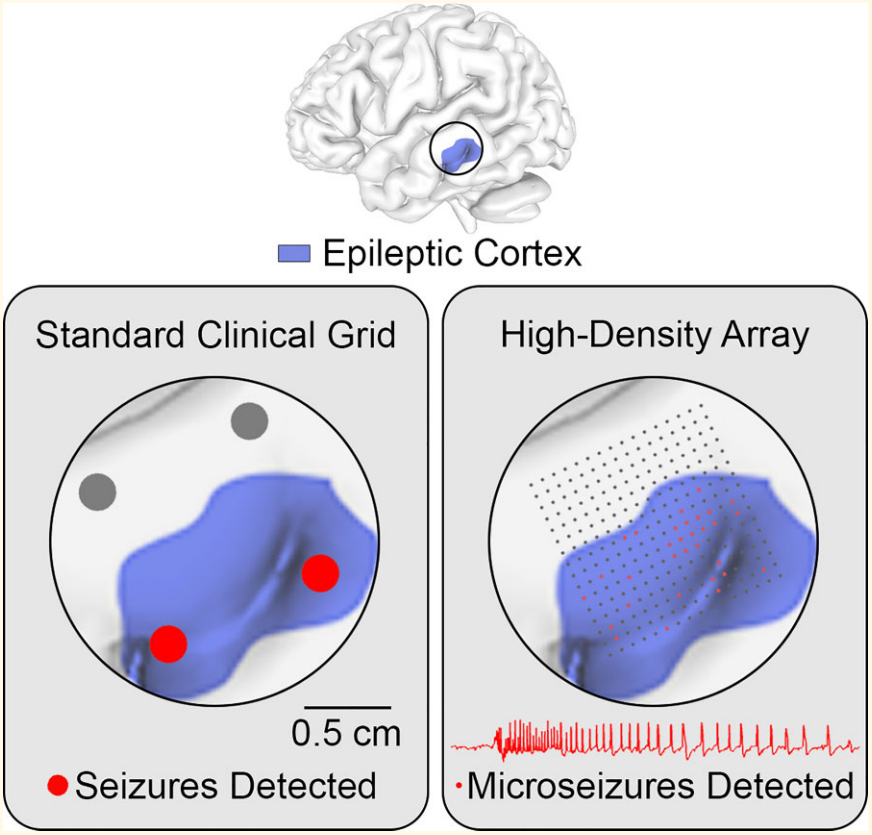

Introduction

Epilepsy affects 1% of the global population, and drugs alone fail to control seizures in ~30% of cases.[1,2] Despite the continued development and approval of novel anti-seizure medications, the high prevalence of drug-resistant epilepsy has persisted for several decades.[2–4] Some patients with drug-resistant, focal-onset epilepsy benefit from surgical resection or ablation of epileptogenic tissue.[1,5–7] Although this treatment is a valuable alternative, surgical resection yields complete postoperative seizure freedom in 30–70% of patients, depending on factors such as a patient's neuropathology, the presence, type and localization of structural lesions, as well as the timing and extent of resection.[4,6] Resective and ablative surgeries also carry risks of postoperative neurocognitive deficits that are in part related to the amount of tissue resected.[4,8] Furthermore, focal epilepsy patients are not candidates for surgical resection or ablation if they exhibit widespread or multifocal epilepsy networks, overlap of epileptogenic cortex with eloquent brain areas, or serious medical comorbidities.[4] Neuromodulation therapies such as responsive neurostimulation (RNS), deep brain stimulation (DBS) and vagal nerve stimulation offer alternatives for these patients but seldom produce lasting seizure freedom.[4,9,10]

Resection, ablation (e.g. laser interstitial thermal or radiofrequency ablation) and RNS require precise targeting of the

epileptogenic zone (EZ)—the brain region for which removal is necessary and sufficient to control seizures.[1,4,11–14] Diagnostic tools currently used to identify the EZ include neuroimaging, seizure semiology, scalp EEG, electrocorticography (ECoG) and stereo-electroencephalography (sEEG).[1,12,15] However, these tools suffer from a lack of spatial precision.[16–19] Invasive neurophysiological techniques such as ECoG and sEEG record aggregate activity from ~3 to 19 mm^2 of tissue, including local neuronal firing, intrinsic currents and synaptic potentials from near and distant sources.[20,21] Spatially localized epileptiform activity on the submillimeter scale is not apparent in standard clinical recordings but has been revealed by experimental recordings from epileptic patients using silicon shank microelectrode arrays and surface and intraparenchymal microwire electrode arrays.[16,22] Recordings in epileptic patients using these arrays have identified seizure-like discharges isolated to single 40-µm diameter wire contacts, termed 'microseizures'.[16,22] These microseizure discharges sometimes evolve into clinical seizures involving multiple square centimetres of cortex.[16,22] One study showed that microseizures occurred at an elevated rate in patients with epilepsy as compared to control patients.[16] While the presence of spontaneous microseizures indicates that ictal activity may begin at the microscale, the spatiotemporal dynamics of these events across larger areas of tissue (144–798 mm^2) and the relevance of these events to the organization of the EZ remain unknown.

One limitation of microarrays that have previously been used to detect microseizures is their minimal coverage of the cortical surface. Here we leveraged advances in micro-electrocorticography (µECoG) electrode arrays with broad, high-density microcontact coverage to study the microscale dynamics of epileptiform activity in human epilepsy patients.[23] For controls, we performed µECoG electrode array recordings in movement disorder patients undergoing DBS surgery. We hypothesized that microseizures occur more frequently in epileptic subjects than in non-epileptic subjects and that most microseizures are spatially restricted to <1–2 mm^2, thus precluding their detection by standard clinical recording electrodes. Our µECoG electrode arrays were minimally invasive and consisted of a flexible liquid crystal polymer thin-film (LCP-TF) substrate with electroplated gold (Au) or platinum–iridium (PtIr) microcontacts.[23] The scale and configuration of the LCP-TF c electrode arrays offered high-density microscale recordings (0.762–1.72mm spacing) while maintaining adequate spatial coverage of the cortical surface (144–798 mm^2), an important compromise between the two spatial extremes of clinical ECoG arrays (10 mm spacing, 6400 mm^2 coverage) and silicon shank microelectrode arrays (0.4 mm spacing, 16 mm^2 coverage).[21,22] The LCP-TF fabrication method created a smooth array surface which minimized the possibility of tissue damage due to surface penetration, which occurs when using silicon shank or microwire electrodes.[23] Our objectives were to determine whether microseizures can be readily observed in brief intraoperative recordings, to assess the specificity of microseizures for epileptic brain, to characterize the spatial scale of detected microseizures and to determine whether microelectrode recording devices are necessary for their detection. Our results indicate that microseizures observed using LCP-TF µECoG electrode arrays may provide a more precise tool to improve presurgical evaluation for drug-resistant epilepsy.

Materials and methods

Participants

We performed intraoperative recordings in nine patients (three females; mean age = 39.1 year; range 29–49) with drug-resistant epilepsy undergoing surgical resection or electrode removal after preoperative intracranial monitoring. As a control, we also recorded intraoperatively from the cortex of four patients with movement disorders undergoing awake DBS surgery (two female; mean age = 65 years, range 61–74). Informed consent was obtained from all patients in accordance with the Institutional Review Boards at New York University Langone Health and the Duke University Health System.

Liquid crystal polymer micro-electrocorticography arrays

LCP µECoG arrays were fabricated by Dyconex AG, Micro Systems Technology (Bassersdorf, Switzerland). The arrays have passed International Organization of Standardization 10993 biocompatibility tests for haemolysis, cytotoxicity and material-mediated pyrogenicity at a contract research organization for medical devices (NAMSA; Toledo, USA) following FDA Good Laboratory Practice regulations. We used LCP-TF arrays with three different designs: 128 microcontacts with 1.33 mm centre-to-centre spacing (pitch), 244 microcontacts with 0.76 mm pitch and 256 microcontacts with 1.72 mm pitch (Fig. 1A).[23] All microelectrode contacts were 200 µm in diameter. The backs of the LCP-TF arrays were coated in polydimethylsiloxane (Dow Corning MDX4-4210, USP Class VI) to allow for mechanical configuration of the arrays and to prevent possible tissue damage by the thin edges of the LCP-TF (Fig. 1C).[23,24] The 128-contact design was sufficiently narrow to permit subdural implantation via a burr-hole during DBS surgery for movement disorders. Electrodes were connected to custom modular headstages with Intan Technologies RHD chips for amplification and digital sampling at 20 kilo samples per second (kSPS) (Fig. 1B). The array, headstages and cabling were sterilized with ethylene oxide gas at Duke or with hydrogen peroxide solution at NYU.

Intraoperative recordings

Recording procedures in the operating room were developed with input from neurosurgeons and neurologists. Craniotomies, burr-hole placement and all other surgical procedures were performed solely for standard of care clinical purposes. Intraoperative recordings from epilepsy patients were collected after intracranial electrode monitoring for

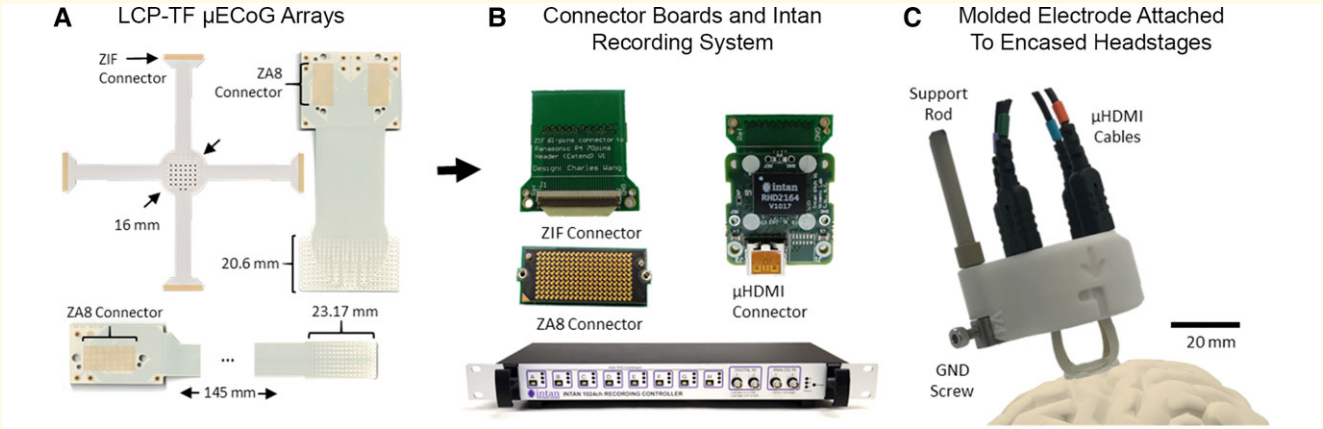

Figure 1 LCP-TF electrodes and intraoperative recording system. (**A**) Flexible LCP electrodes with 244 (left), 256 (right), and 128 (bottom) Au recording contacts [200 µm diameter; pitch = 0.762 mm [left], 1.72 mm (right), 1.33 mm (bottom)]. (**B**) Custom digitizing headstage using an Intan Technologies integrated circuit. Electrode arrays were connected to the digitizing headstage using either Zero Insertion Force (ZIF) or Samtec ZA8 adaptor printed circuit boards. The Intan Technologies recording controller collected digital signals from the headstages. (**C**) Example of an LCP-TF electrode array moulded in silicone and attached to four headstages inside a 3D-printed support structure with µHDMI cables for connection to the recording controller. Schematic depicts electrode placement on the cortex.

presurgical evaluation had taken place in 7/9 patients. In these cases, the neurosurgeon placed a sterilized LCP-TF array on the cortical surface closest to the area of seizure onset or early spread (defined as within 5–15 s) identified by a neurologist (Fig. 1C, Supplementary Fig. 1). In two patients (P3 and P9), intracranial electrode monitoring was not performed because a clear lesion was identified on the MRI and presumed to be the epileptogenic focus. In patient P3, the neurosurgeon placed the array as close to the lesion as possible within the constraints of the edge of the craniotomy. In patient P9, the array was placed on the cortical surface directly on the lesion. During intraoperative recordings from patients undergoing awake DBS surgery, the neurosurgeon slid a 128-contact array through a burr-hole and onto the cortical surface (Supplementary Fig. 2). Sterile alligator clips connected the ground and reference terminals of the headstages to an accessible metal connection on the patient's body such as a metal scalp retractor or bone screw. Headstages were connected by micro high-definition multimedia interface (µHDMI) cables to an Intan Technologies recording controller that was positioned outside the sterile zone. Recordings were conducted when patients were either anaesthetized or awake during intraoperative mapping of eloquent cortex or motor control (Table 1).

Data preprocessing

Neural data was recorded at 20 kSPS, low-pass filtered using a multitaper filter with a time window of 0.01 s and frequency bandwidth of 300 Hz and downsampled to 1 kHz. Channels with high impedance (>250 kΩ at 1 kHz on postoperative testing) and epochs with excessive artefact (based on visual inspection) were excluded from analysis.

Data analysis

A line length (LL) detector was used to screen recordings for candidate events.[25] LL was calculated over an interval of 1000 samples (a 1 s window) in steps of 500 ms. A candidate event was flagged each time LL exceeded 1.5 × median for each channel. A total of 28 645 candidate events were identified.

Multitaper spectral estimation using a sliding 200 ms window with 10 ms steps and 5 Hz smoothing was performed to construct spectrograms to visualize µECoG frequency changes over time. Spectrograms were then z-scored to normalize power across each channel. Filtered voltages, voltages with local re-referencing (subtraction of mean voltage of neighbouring channels) and normalized spectrograms were evaluated by a board-certified epileptologist (D.F.) and a trained reviewer (J.S.). Events were labelled as microseizures if they were deemed by both reviewers to have met three criteria[16]: (i) paroxysmal start from baseline, (ii) evolution in frequency over time and (iii) return to baseline.

To quantify the evolution of frequency over the course of an event, the maximum frequency was plotted against time. The maximum frequency over a time bin t for a power spectral estimate $P(f)$, where f is frequency, is defined as:

$$\text{Frequency Max}_t = \text{argmax}(\log_2(P(f))). \quad (1)$$

The rate of frequency change for a given event was calculated as the difference in Frequency Max at the start and end of the event divided by the duration. Events were determined to be increasing or decreasing in frequency by the slope of the least squares regression line of Frequency Max over the course of the event.

To investigate the effect of contact size on microseizure detection, voltages on adjacent electrodes on the 244-channel

Table 1 Clinical summary of patients

Patient	Age	Sex	Diagnosis	Array location	Recording duration	Channels	Awake status	Anaesthesia/analgesia
1	41	F	Focal epilepsy	L posterior superior temporal gyrus	18 m 10 s	256	Anaesthetized	Isoflurane (0.8%)
2	34	M	Focal epilepsy	L posterior superior temporal gyrus	18 m	244	Awake	Remifentanil (0.02 mcg/kg/min)
3	37	M	Focal epilepsy	L posterior superior temporal gyrus	8 m 50 s	256	Awake	
4	39	M	Focal epilepsy	L temporal pole	6 m	244	Anaesthetized	Propofol (50 mcg/kg/min) Remifentanil (0.1 mcg/kg/min) Dexmedetomidine (0.2 mcg/kg/hr)
5	41	F	Focal epilepsy	L precentral gyrus	5 m 28 s	244	Anaesthetized	Sevoflurane (1.64%) Remifentanil (0.05 mcg/kg/min) Dexmedetomidine (0.2 mcg/kg/hr)
6	49	F	Focal epilepsy	L anterior middle temporal gyrus	10 m 40 s	244	Anaesthetized	Propofol (130 mcg/kg/min) Remifentanil (0.125 mcg/kg/min)
7	29	M	Focal epilepsy	R posterior superior temporal gyrus	5 m	244	Anaesthetized	Propofol (100 mcg/kg/min) Remifentanil (0.1 mcg/kg/min)
8	35	M	Focal epilepsy	L middle temporal gyrus	6 m	244	Anaesthetized	Propofol (25 mcg/kg/min) Remifentanil (0.03 mcg/kg/min) Dexmedetomidine (0.3 mcg/kg/hr)
9	47	M	Focal epilepsy	L posterior temporal gyrus	16 m 30 s	2 × 256	Awake	
10	62	F	Movement disorder	L prefrontal cortex	53 m 40 s	128	Awake	
11	74	F	Movement disorder	L motor cortex	7 m 35 s	128	Awake	
12	61	M	Movement disorder	L motor cortex	10 m	128	Awake	
13	63	M	Movement disorder	R motor cortex	8 m	128	Awake	

array were averaged to simulate larger electrodes. The LL ratio—the LL over a short-term window (the preceding 1 s) divided by a long-term window (the preceding 60 s) calculated in steps of 50 ms—was used to illustrate the sensitivity of microseizure detection at different contact sizes.[13,25] The microseizures at each contact size were labelled as described above based on spectrograms that were constructed using the averaged signal. To investigate the effect of contact spacing on microseizure detection, electrodes on the 244-channel array were removed to simulate arrays of varying pitch. The microseizures on the remaining channels were then identified. When available, features of each subject's microseizures were compared with the macroseizures captured during clinical preoperative monitoring using standard sized sEEG or ECoG grid electrodes. Specifically, for each microseizure and macroseizure event, the mean Frequency Max across the entire event duration was computed.

Statistical analysis

Multiple statistical tests were performed to assess whether the microseizure rate in awake and anaesthetized epilepsy patients differed. A two-sided permutation test ($n = 10\,000$ permutations) was used to test for a difference in means; a two-sided Mann–Whitney U test was used to test for a difference in ranks; and a two-sided Kolmogorov–Smirnov test was used to test for a difference in distributions. To assess whether the microseizure rate in the recordings of epilepsy patients (pooled across awake and anaesthetized patients) was higher than the microseizure rate in the recordings obtained in movement disorder patients, one-sided permutation ($n = 10\,000$), Mann–Whitney U and Kolmogorov–Smirnov tests were used. A one-sided permutation test ($n = 10\,000$) was performed to test the null hypothesis that the mean power in the low-frequency (<30 Hz) or high-frequency (70–150 Hz) band for a single channel was higher than the mean power across all channels involved in the event. A two-sided permutation test was used to compare mean Frequency Max values between microseizures and macroseizures for each patient and across all patients and a two-tailer Fisher's exact test was used to compare the proportion of microseizures and macroseizures with increasing and decreasing Frequency Max. Significance for all tests was defined as $P < 0.05$. For multiple comparisons, the Benjamini-Hochberg procedure for controlling the false discovery rate was used with an alpha value of 0.01. Statistical analyses were performed using MATLAB 2021a (MathWorks, Inc.; Natick, MA).

Data availability

Data obtained in this study are available upon request. Please contact the corresponding authors with any inquiries.

Results

We performed intraoperative recordings using μECoG arrays (median duration: 7.6 min, range: 5.0–53.7 min) in nine patients with focal epilepsy and four patients without

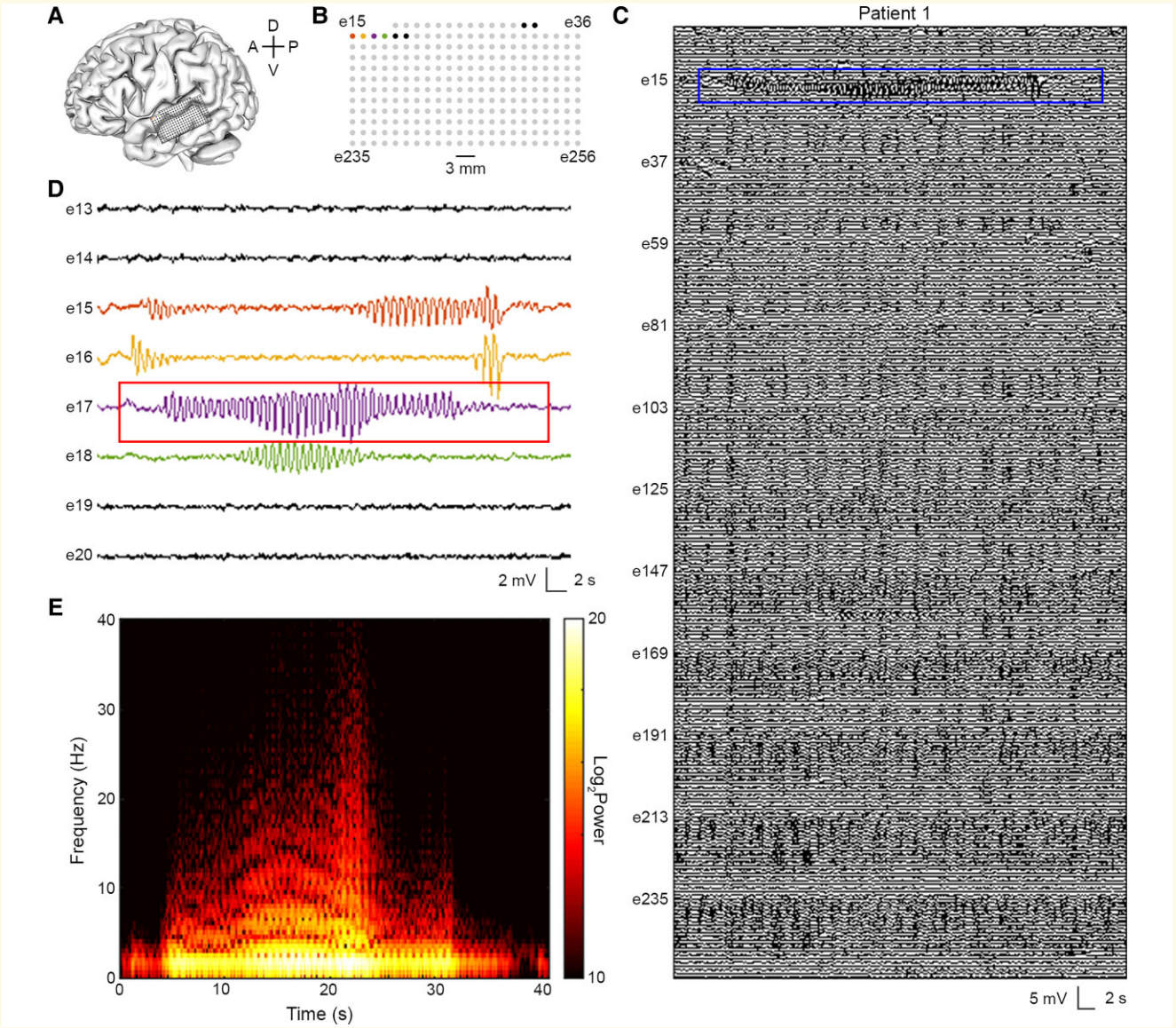

Figure 2 A high-density μECoG array enables detection of electrographic seizure activity limited to single electrodes. (**A**) Schematic of array recording location in patient P1. A, anterior; P, posterior; D, dorsal; V, ventral. (**B**) Map of electrode contacts in 256-channel array. Coloured contacts correspond to single channels where microseizure events were detected. (**C**) μECoG signal across all 256 channels. Blue outline delineates zoom window shown in panel D. (**D**) μECoG signal showing electrographic seizure activity in electrodes 15, 16, 17, and 18. Red outline delineates spectrogram window shown in panel E. (**E**) Spectrogram of the microseizure event found on electrode 17. The event demonstrates hallmarks of electrographic seizure activity: paroxysmal change from background, temporal and spectral evolution, and discrete termination.

epilepsy (Table 1). Fig. 2 shows representative recordings from the left posterior superior temporal gyrus of a patient with focal-onset epilepsy (P1), obtained using the 256-channel μECoG array. As in previous reports of extra-operative recordings performed in awake patients,[16,22] we identified microseizures that localized to single electrodes in an anaesthetized patient (Fig. 2B–E). Unexpectedly, we found that the microseizures occurred in close spatial and temporal proximity (Fig. 2B,D). We confirmed with time-frequency analysis that the detected microseizures displayed the stereotypical characteristics of an electrographic seizure: (i) paroxysmal start, (ii) spectral evolution and (iii) return to baseline (Fig. 2E).

Of the candidate events identified with the LL detector across 13 recordings in 11 patients, we identified 143 microseizures. Nearly all events (98.6%) occurred in the seven of nine epilepsy patients. We additionally detected two microseizures in a movement disorder patient (P10). The means, ranks and distributions of microseizure rates in awake ($n = 3$) and anaesthetized ($n = 6$) epilepsy patients were not significantly different (permutation test, test statistic = 2.0483, $P = 0.5703$; Mann–Whitney U test, $U_1 = 12.5$,

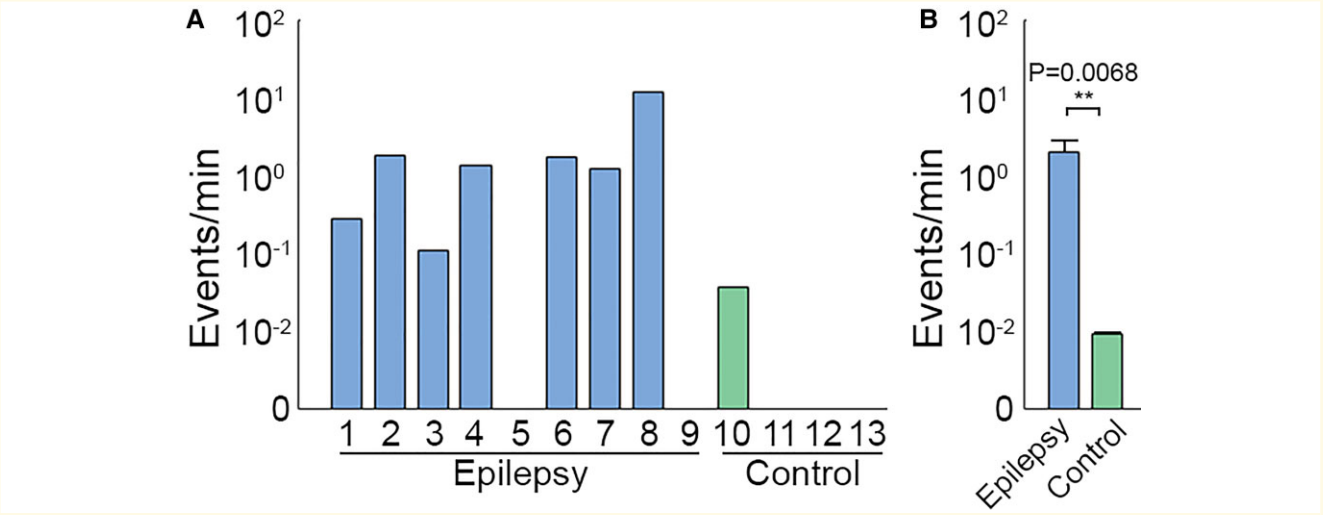

Figure 3 Microseizure rate is higher in clinically identified epileptic brain than in control subjects without epilepsy. (**A**) Microseizure rate observed in epilepsy patients (blue) and in control patients with movement disorder (green). (**B**) Mean microseizure rate observed across all recordings in epilepsy patients ($n = 9$, blue) and across control subjects ($n = 4$, green). Permutation test, $^{**}P < 0.01$.

$U_2 = 5.5$, $P = 0.6190$; Kolmogorov–Smirnov test, $D^* = 0.5$, $P = 0.5344$) (Supplementary Fig. 3); therefore, we pooled recordings from awake and anaesthetized epilepsy patients into a single group. The microseizure rate from epilepsy recordings ($n = 9$) was significantly higher than in non-epileptic controls ($n = 4$) in means, ranks and distributions (2.01 versus 0.01 microseizures/min, permutation test, test statistic = 2.0028, $P = 0.0068$; Mann–Whitney U test, $U_1 = 5$, $U_2 = 31$, $P = 0.0210$; Kolmogorov–Smirnov test, $D^* = 0.7778$, $P = 0.0159$) (Fig. 3B). These results suggest that the presence of microseizures may serve as a potential biomarker for epileptic brain.

We identified diverse spatial and temporal patterns of microseizure activity in epilepsy patients (Fig. 4). Microseizures involving multiple adjacent channels were found (Fig 4A–J), in addition to events detected on a single channel (Fig 4K–O). The mean number of channels involved per microseizure event was 3.0 (standard deviation: 5.8, range: 1–29). Events also varied in duration, for example the microseizure shown in 4C lasted ~7.5 s, whereas the microseizure displayed in 4H was only 300 ms in length. The mean microseizure duration was 5.91 s (standard deviation: 11.4 s, range: 0.2–106.6 s). Quantification of frequency evolution over the course of these events revealed distinct patterns (Fig. 4E,J,O). Frequency Max changed at a rate of −15.3, 159.7 and −7.8 Hz/s for the microseizures in patients P7, P4 and P8, respectively.

We next sought to determine the extent to which contact size and density contributed to microseizure event detection. We simulated recordings from virtual electrodes with contact diameters of 1.7, 2.4 and 3.2 mm by spatially averaging the signals from d electrodes (Fig. 5A). Fig. 5B shows an example of an isolated microseizure event and voltages from virtual electrodes of varying sizes. When LL ratio was calculated for each of these four signals, only the LL ratio for the 200 μm contact exceeded 1.75, a commonly used threshold for clinical detection (Fig. 5C). Since conventional macroelectrode grids have a contact diameter of 2.3 mm, this example highlights the potential for electrodes with large contact sizes to fail to detect highly focal events, such as microseizures. The mean Frequency Max across all 143 microseizure events was 25.3 ± 5.0 Hz compared with 8.9 ± 0.5 Hz for 41 clinical macroseizures captured during preoperative monitoring (two-sided permutation test, $P = 0.0458$, Supplementary Fig. 4). These results indicate the ability of microelectrodes to capture higher frequency epileptic activity. In addition, we found that 70/143 (49.0%) of microseizures were associated with increasing Frequency Max, which was significantly greater than the 10/41 (24.4%) of macroseizures with increasing Frequency Max (two-tailed Fisher's exact test, $P = 0.0025$).

We analyzed virtual recordings across five epilepsy patients (P2, P4, P6, P7, P8) of all 135 microseizure events acquired using the highest-density 244-channel μECoG array. We found that the number of microseizures detected by virtual electrodes declined with increasing simulated contact diameter: 46 (1.7 mm contact diameter), 19 (2.4 mm) and 11 (3.2 mm), from the set of 135 events (Fig. 5D). Our data suggest that ~86% of microseizures fail to be detected at 2.4 mm, the contact diameter closest to macroelectrodes used in conventional clinical subdural grids. As expected, events that were detected on 1-2 contacts exhibited the sharpest decrease (93.6%) from 0.2 to 2.4 mm contact diameter (109–7 microseizures), whereas events that were more spatially distributed (i.e. appeared on >5 contacts) were more likely to be captured with electrodes with larger simulated contact sizes (Fig. 5E). We also performed analyses to investigate the effect of contact density on microseizure event detection (Fig. 5F). By removing channels from our analysis, we simulated recordings from arrays with increased contact

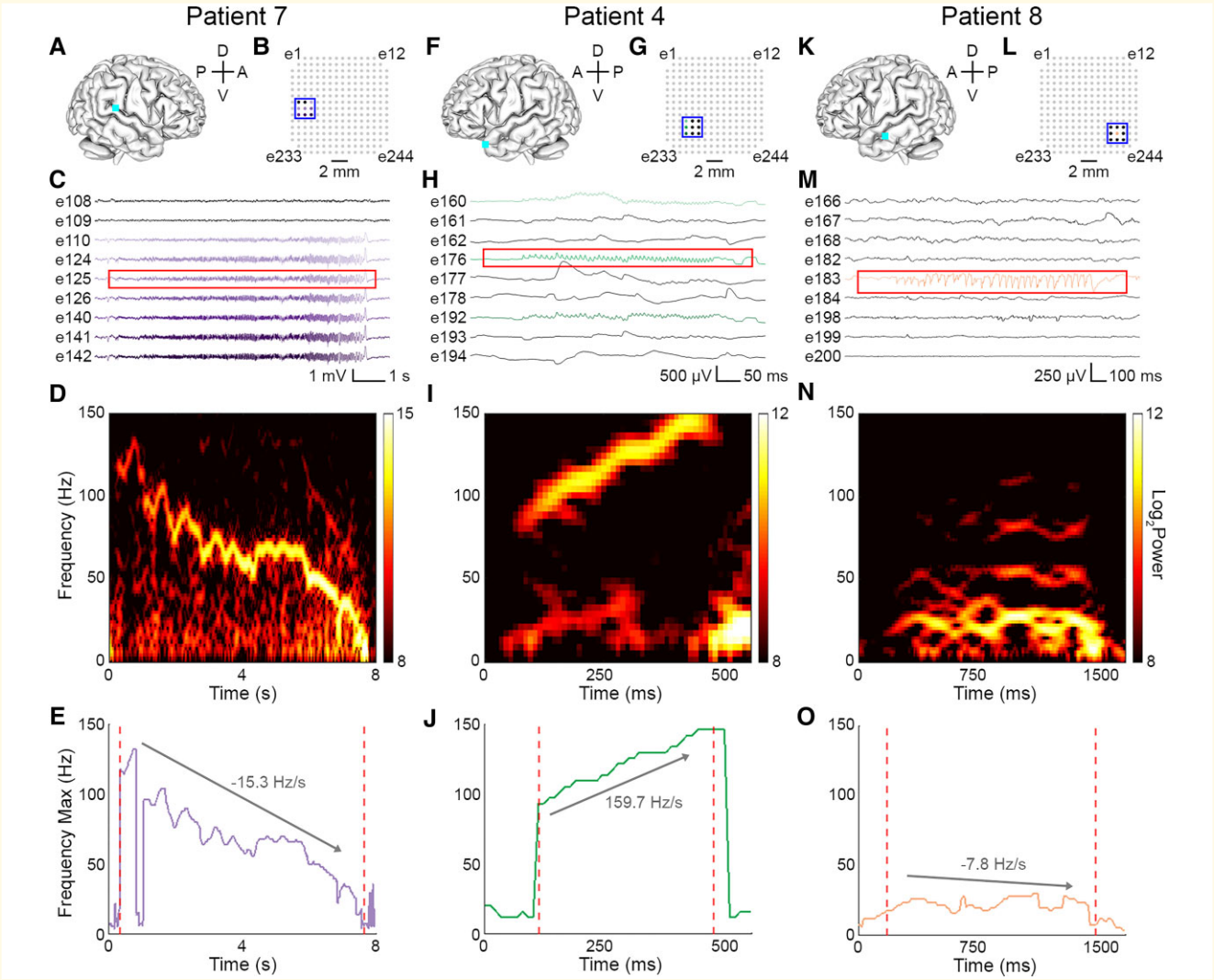

Figure 4 Microseizures in epilepsy patients vary in spatial extent, duration, and frequency. (**A, F, K**) Schematic of array recording location (cyan square) in patients P7 (A), P4 (F) and P8 (K). A, anterior; P, posterior; D, dorsal, V, ventral. (**B, G, L**) Map of electrode contacts in 244-channel array. Coloured contacts correspond to single channels where microseizure events were detected. Blue outline delineates the channels whose traces are shown in panels C, H and M. (**C, H, M**) μECoG signal showing microseizures. Coloured traces indicate channels where events were detected. Red outline delineates spectrogram window shown in panels D, I and N. (**D, I, N**) Spectrograms of the microseizures boxed in red in panels C, H and M. (**E, J, O**) Frequency Max of microseizures displayed in panels D, I and N. Dotted red lines indicate start and end of microseizure. Labelled arrow shows change in Frequency Max from start to end of event.

spacing. Consistent with the presence of a spatially-focal event, the number of detected microseizure events decreased with increasing contact spacing: 86 events (1.08 mm spacing), 59 (1.52 mm), 33 (2.15 mm), 21 (3.05 mm) and 17 (4.31 mm), out of a total of 135 events observed on the full array.

Finally, we asked whether the μECoG array could identify the putative focus of spatially distributed events. Of the 143 microseizure events detected, nine (6.3%) occurred simultaneously on more than five contacts. We show one example in patient P4 that was recorded across eight channels (Fig. 6A–C). We first analyzed the low-frequency power (<30 Hz), a frequency range traditionally used by clinicians to identify electrographic seizure activity (Fig. 6D). Low-frequency local field potential (LFP) power (normalized to a 5 s baseline period) in two electrodes, e176 and e192, was significantly greater than the mean across all eight electrodes (e176: test statistic = 0.1131, $P < 1e\text{-}4$, e192: test statistic = 0.0353, $P < 1e\text{-}4$; random permutation test). Multiple sources contribute to low-frequency LFPs; however, the high-frequency extracellular potential is known to reflect locally-generated neural activity.[26] Therefore, we also examined power in the high-gamma band (70–150 Hz) (Fig. 6E). Electrodes e176 and e192 had significantly elevated high-gamma power compared to the mean across all eight electrodes (e176: test statistic = 0.2010, $P < 1e\text{-}4$, e192: test statistic = 0.0864, $P < 1e\text{-}4$; random permutation test). This result further supports the idea that the putative focus

of the microseizure event is spatially localized and near the two recording sites (Fig. 6F).

Discussion

Our results show that microseizures are a phenomenon specific to epileptic brain and can be detected using high-density μECoG arrays during brief intraoperative recordings. We found that high-density μECoG arrays with broad spatial coverage can detect microseizures that occur in the absence of clinical seizures in both anaesthetized and awake epilepsy patients. Detected microseizures had variable frequency dynamics, duration and spatial extent, and occurred more frequently in epilepsy patients than in controls ($P = 0.0068$; Fig. 3). Our results also suggest that standard clinical arrays would not have detected most microseizure events (Fig. 5). Specifically, spatial averaging and subsampling simulations indicated that increases in contact size and spacing would result in fewer detectable microseizure events across all recordings. This suggests that μECoG arrays with small contacts, high contact density and large coverage are crucial to capturing microseizure activity. We also demonstrated the utility of μECoG arrays to localize possible foci of microseizures occurring across an area of multiple channels based on differences in low frequency (<30 Hz) and high-gamma (70–150 Hz) signal power between contacts (Fig. 6). In addition, we found that on average, microseizures had a higher Frequency Max than macroseizures (Supplementary Fig. 4). Together, our findings show that microseizures are specific to epileptic brain and that high-density μECoG arrays with broad spatial coverage are essential to their detection.

Our μECoG arrays offer several strengths that enabled the capture and spatiotemporal analysis of microseizures in the human brain. A crucial advantage is the balance between spatial resolution (contact size and density) and spatial coverage. Most prior research on seizure activity in human subjects has used data collected from either clinical grids with coarse spatial resolution (10 mm pitch) but extensive spatial coverage (on the order of 6400 mm^2), or very high-resolution microelectrode arrays with limited coverage, such as Utah arrays with penetrating silicon shanks (0.4 mm pitch, 16 mm^2 coverage) or the cut tips of microwires (1 mm pitch, ≤10 clusters of ≤16 mm^2 coverage each) protruding between standard clinical grid or sEEG electrode contacts.[16,22] Here we describe devices and methods that yield microscale recordings while maintaining extensive spatial coverage comparable to clinical grid arrays. Although the contact size and spacing of our μECoG devices do not allow for the study of microseizures in relation to spiking activity as captured by penetrating microelectrode arrays, our spatial coverage and standard ECoG signal analysis methods may enable more direct and intuitive clinical translation of our results. Another key advantage of using these arrays is the choice of the LCP-TF material and electroplated Au and PtIr microcontacts. Our flexible LCP-TF electrode arrays better conform to the curvature of the cortex than penetrating microelectrode arrays and have smoother surfaces, offering higher signal-to-noise and increased protection of brain tissue. Previous work using penetrating arrays or cut wire tips has received some scrutiny due to the similarity between reported microseizures and electrographic signals resulting from cortical injury.[27,28] The smooth surface of our μECoG arrays mitigates this concern, providing greater confidence that the microseizures captured in our recordings are truly electrographic events and not a result of tissue damage.[23] The intrinsic strengths of our LCP-TF μECoG arrays, as well as the small contact size, high contact density and broad coverage, are critical to the safe and specific detection of microseizures.

Interestingly, the occurrence of microseizures in microarray recordings has varied between studies and devices. Using penetrating platinum-coated silicon microelectrodes with 3–5 μm tips spaced 400 μm apart, Schevon et al.[22] found microseizures in three of five epileptic patients (60%). Using an array of 30-μm diameter poly(3,4-ethylenedioxythiophene) polystyrene sulphonate contacts spaced 50–600 μm apart, Yang et al.[19] observed microseizure activity in only 1 of 30 epilepsy patients (3%). In contrast, Stead et al.[16] used the cut ends of PtIr wire as electrode contacts (40 μm diameter and 0.5–1 mm spacing) and observed microseizures in 14 of 14 epilepsy patients (100%). Although we used devices with larger contact diameter (200 μm) and larger spacing (0.762–1.72 mm) than in these previous studies, our devices also provided the largest coverage (144–798 mm^2). We observed microseizures in seven of nine epilepsy patients (78%), and these events were detected at an average rate of 2.01 events/min (Fig. 3). The event frequency we observed is greater than previously reported in a similar study[16] (0.014 microseizures/min). This variability in microseizure frequency between studies may be due to differences in the brain regions recorded, patient disease states, microelectrode array coverage and pitch, microseizure detection during visual review, anaesthetic regimens and states of anaesthesia and wakefulness. For example, some anaesthetics such as remifentanil and sevoflurane may promote interictal epileptiform activity while others such as isoflurane may suppress interictal epileptic activity.[29] We recorded from patients under various anaesthetics including remifentanil, sevoflurane and isoflurane (Table 1). However, we did not find a significant difference between the frequency of microseizures in epileptic patients under anaesthesia at the time of recording and epileptic patients who were awake (Supplementary Fig. 3). Further work recording at high resolution across a variety of epileptic pathologies is needed to better understand the variability in microseizure occurrence between patients and to better identify the smallest region within which clinically relevant microseizure events occur.

A key result of our analysis is that clinical macro contacts would be unlikely to detect the majority of microseizure events recorded by our LCP-TF μECoG arrays. LFP signals captured by metal contacts placed on the brain surface predominantly reflect a summation of postsynaptic currents in

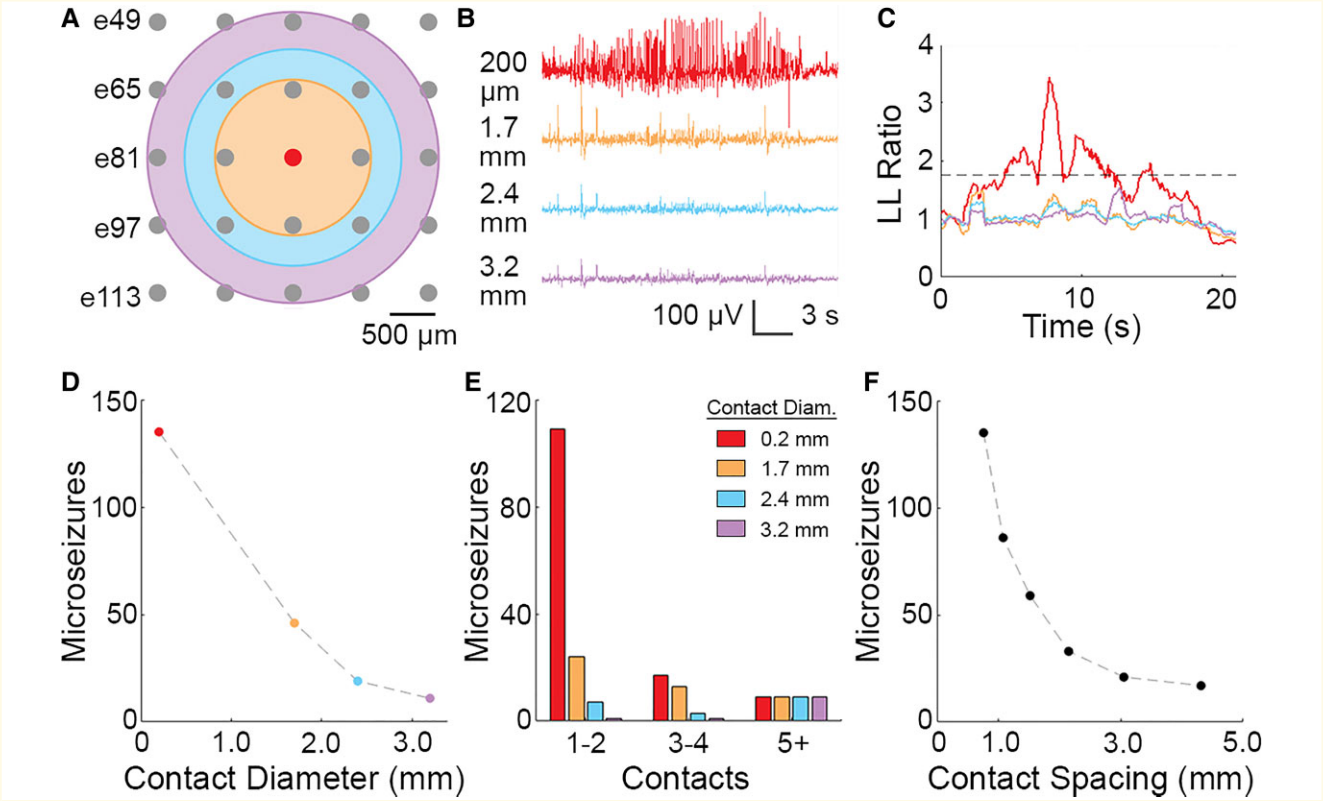

Figure 5 Increased spatial resolution via smaller contacts at greater density facilitates microseizure detection. (**A**) Map of electrode contacts in 244-channel μECoG array. Spatially averaged electrodes with diameters of 1.7 mm (orange), 2.4 mm (blue) and 3.2 mm (purple) are shown. (**B**) Example of a spatially averaged μECoG signal shown in colours corresponding to electrodes from panel A. Red trace highlights the microseizure event isolated to a single channel. (**C**) LL ratio for the spatially averaged traces in panel B. Dotted line shows threshold LL ratio of 1.75. (**D**) Total number of microseizures detected by 244-channel arrays at various contact diameters. Colours correspond to electrode schematic in panel A. (**E**) Total number of microseizures detected at various contact diameters, grouped by the number of contacts per microseizure. (**F**) Total number of microseizures detected by 244-channel arrays at different spacing widths (centre-to-centre).

mostly superficial cortical layers.[20,26] Larger contacts measure an average of activity across a greater number of neuronal sources. We simulated the signal that larger contacts would measure during microseizures by averaging signals captured between multiple microcontacts in our recordings. While some features of the signal are visible across spatial scales, the microseizure quickly becomes undetectable when larger contacts are simulated. When simulating the signal captured over a 2.4 mm diameter area, a size comparable with clinical-standard 2.3 mm diameter contacts, we detected 86% fewer microseizures than when using 200 μm diameter contacts. Although spatial averaging between microcontacts is a reasonable approximation, it is not necessarily equivalent to the signal that would be measured by a larger solid contact. Specifically, our simulated result does not account for the LFP signal between the microcontacts or the decrease in impedance and change in signal-to-noise ratio when using a contact with greater surface area. However, assuming that the electric field in the <300 Hz frequency range is smooth between recording sites, our spatial averaging analysis provides a useful proxy for the signal observed when using larger area contacts.[30] This result is notable given that the majority (81%) of microseizures detected in our recordings occurred on only one or two contacts at a time. We also found that the mean Frequency Max across all microseizures (25.3 ± 5.0 Hz) was higher than the mean Frequency Max of macroseizures (8.9 ± 0.5 Hz, $P = 0.0458$)) and that Frequency Max increased over time in a greater proportion of microseizures (51.0%) than clinical macroseizures (24.4%, $P = 0.0025$; Supplementary Fig. 4). This result may reflect the ability of microcontacts to better capture spatially restricted, high-frequency seizure events compared with clinical macroelectrode contacts. These results also suggest the possibility of different pathological circuits and ictogenesis reflected by microseizure and macroseizure events. Further work is needed to identify the physiological mechanisms underlying seizure activity at various scales.

We also found that the density of microcontacts was critical to detecting microseizure events (Fig. 5). By subsampling the array, we were able to simulate recordings of varying contact spacing and observed that fewer microseizures were detected as contact density decreased. More notably, the decline in the number of microseizure events detected

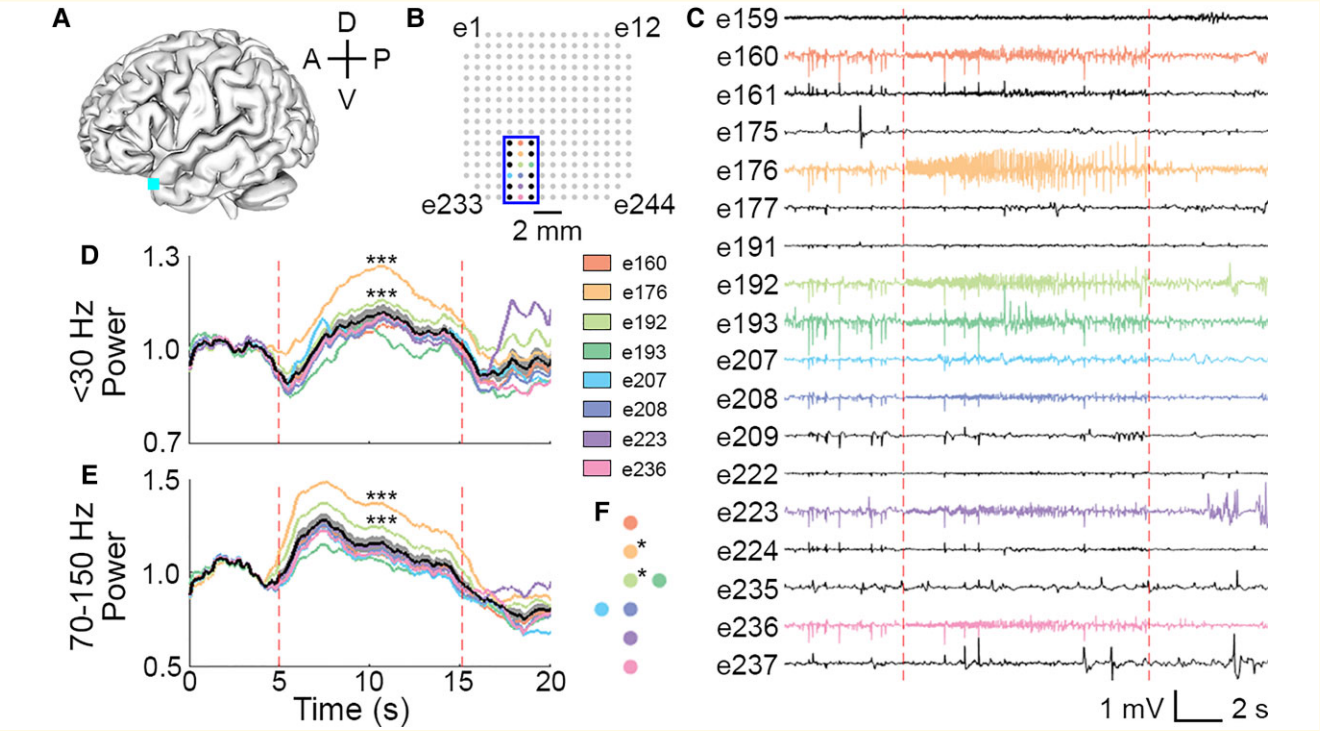

Figure 6 Spectral analysis of a spatially distributed event highlights potential to identify the focus of activity within a microseizure. (**A**) Schematic of array recording location (cyan square) in patient P4. A, anterior; P, posterior; D, dorsal; V, ventral. (**B**) Map of electrode contacts in 244-channel array. Coloured contacts correspond to single channels where microseizures were detected. Blue outline delineates the channels whose traces are shown in panel C. (**C**) μECoG signal showing microseizures in P4. Coloured traces indicate channels where events were detected. Dotted red lines indicate start and end of event. (**D**) Low-frequency (<30 Hz) and (**E**) high-gamma (70–150 Hz) power derived from summed multitaper spectral estimates of the μECoG signal shown in C, normalized to the baseline period of 5 s preceding the start of the microseizure. The mean power of the eight coloured traces (±SEM) is shown in black (grey shading). Permutation test, ***$P < 0.0001$. (**F**) Map of electrode contacts where microseizures were detected. Asterisks (*) signify electrodes which had significantly elevated power compared with the mean.

(from 135 to 86 events) between 0.76 mm and 1.08 mm contact spacing suggests that an even greater density of contacts (<0.76 mm spacing) could result in a substantial increase in the number of detected microseizure events. These results support our hypothesis that μECoG arrays capture epileptic events that would not be observed using standard clinical grids. Determining the smallest spatial scale needed to capture all microseizure events requires further microscale study of epileptic cortex, along with technology development and biophysical modelling of μECoG recordings.[31,32] As thin-film fabrication and encapsulation of actively multiplexed microelectrode arrays continue to improve, spatial resolution and coverage of recording arrays will increase, enabling more comprehensive recordings of microscale epileptic activity.[33]

Identifying foci of activity within larger seizure events is essential for effective therapeutic targeting. While most microseizure events occurred on only 1-2 channels, we also identified events that were spatially distributed over neighbouring channels (Fig. 6). In such cases, we investigated whether there was an identifiable focus of activity. Traditionally, epileptologists have assessed low-frequency features (<30 Hz) of ECoG recordings to identify seizure activity. However, recent work has demonstrated that high-gamma LFP signals (70–150 Hz) reflect more spatially localized spiking activity.[34,35] In the case of spatially distributed microseizures in our recordings, particular channels had signal power within both these frequency ranges that was significantly elevated compared to the mean across neighbouring channels involved in the microseizure. We hypothesize that the channels with higher signal power, especially in the high-gamma frequency range, are distinctly active within the distributed microseizure events and thus could be a more optimal therapeutic target, especially in the case of micro-stimulation.

Some limitations of the current study can be addressed by future work. For example, we gathered only brief intraoperative recordings, often while the patient was anaesthetized (Table 1). This experimental set-up limits our ability to relate these intraoperative microseizures with macroscale seizures captured during awake clinical monitoring. However, the ability to capture microseizure activity from intraoperative recordings also presents a promising epileptic biomarker which may improve intraoperative mapping of the EZ. With the opportunity to record during semi-chronic

implantation, Schevon et al[22] and Stead et al[16] observed the evolution of microseizures into clinical seizures, thus relating the two phenomena in a meaningful way. Further data collection, particularly recording simultaneously at both the micro- and macroscale with wide coverage during short-term implantation, will be needed to identify the smallest spatial scale at which seizure activity is initiated and propagated.[23] Data from these hybrid-scale recordings would further test our result that most microseizures are undetectable on macrocontacts and would answer questions regarding the relationship between microscale and macroscale seizures and how they may best be interrupted by treatments including resective surgery, laser ablation and RNS. In addition, we have collected microscale recordings only from the surface of the brain; it is not yet known to what extent μECoG recordings reflect activity from deeper neuronal sources. The source of microseizures and their occurrence and propagation among various cortical layers remains unclear. Future work in which laminar depth recordings are conducted simultaneously with microscale surface recordings will be critical to understanding the relationship between microseizures captured at the brain surface and activity from deeper structures.[24] While grids remain a crucial tool for clinical delineation of the EZ in presurgical and intraoperative evaluation, there is expanding use of sEEG electrodes in clinical monitoring due to their improved safety and comfort profiles.[21] Therefore, micro-sEEG devices are also needed to provide additional clinically relevant information on microseizures in epilepsy.[23]

This study and others raise the question as to why microseizures are found not only in epileptic patients but also occasionally in control patients.[16] It may be that microseizures occur spontaneously in non-epileptic brain tissue, but that differences in connectivity or inhibition between neural populations of healthy versus pathologic tissue influence the rate of occurrence and propensity of microseizures to spread into large-scale seizures. There have also been rare cases of cryptogenic epilepsy in Parkinson's patients, so the presence of microseizures in movement disorder patients may reflect an underlying risk for epilepsy.[36] While present, we found only two microseizures in non-epileptic patients compared with 143 microseizures in epileptic patients. Further study is needed to explain the origin of microseizure events in non-epileptic brain tissue.

Our results demonstrate that microseizures occur more frequently in epileptic patients and that high-density microcontact arrays with extensive coverage are crucial to capturing microseizures, as most events would be undetectable on clinical macro contacts. We have successfully identified microseizure events in intraoperative recordings of epileptic and non-epileptic patients using flexible LCP-TF μECoG arrays. We found elevated rates of microseizure events in epilepsy patients and demonstrated the utility of dense, microscale recording arrays to capture these events. Our results contribute to a growing body of evidence that epileptic activity in the human brain is occurring at much finer spatial scales than reflected in clinical-standard ECoG and sEEG recordings. Furthermore, we show variations in high-gamma power between neighbouring contacts during microseizures which differentiate even more specific foci within microseizure events. Since the success of surgical treatments such as resection, laser ablation and RNS are dependent on accurate targeting of seizure initiation sites, precise localization of the EZ is critical to improving outcomes for patients with drug-resistant epilepsy. This work demonstrates the importance of additional research on microscale phenomena in epilepsy, particularly using μECoG arrays with both high resolution and broad coverage. We expect that further research will reveal how microscale biomarkers may be used for differentiating epileptic from non-epileptic tissue in cases of ambiguity, thus improving therapeutic outcomes in refractory epilepsy.

Acknowledgements

We would like to thank the patients who participated in this study, as well as Lora Fanda and Beenish Mahmood, who assisted with data collection at NYU Grossman School of Medicine and Anna Thirakul and Seth Foster, who assisted with data collection at Duke University School of Medicine. We would also like to thank Finding a Cure for Epilepsy and Seizures (FACES) for providing financial support.

Funding

J.S. receives support from the National Institutes of Health (T32 GM136573), the Vilcek Fellowship and the American Epilepsy Society. K.B. receives support from the National Science Foundation (Graduate Research Fellowship Program DGE-1644868). D.F. receives support from the National Institutes of Health (R01 NS06209207, R01 NS109367), the Centers for Disease Control (U48DP006396-01SIP 19-003) and Epitel. O.D. receives support from the National Institutes of Health (R01 MH107396, U01 NS099705, R01 MH111417, U01 NS090415, R01 MH116978, R01 HL151490), Tuberous Sclerosis Alliance, Epilepsy Foundation of American and the National Science Foundation. W.D. receives support from the National Institutes of Health (R01 NS062092, R01 MH116978). S.D. receives support from the National Institutes of Health (RF1 MH116978, R01 MH111417, R01 NS062092), the Office of Naval Research and the Templeton World Charity Foundation. B.P. receives support from the National Institutes of Health (U01 NS099697, U01 NS099577, U01 NS103518, U01 NS122123, R01 NS104923), the Army Research Office (68984-CS-MUR) and the National Science Foundation (IOS-1557886, IIS-2113271). J.V. receives support from the Department of Defense (EP200077), the National Institutes of Health (U01 NS099697, 1UG3NS120172, 1U01NS123668, Clinical and Translational Science Awards grant UL1TR002553) and the National Science Foundation (CBET-1752274). D.S. receives

support from the National Institutes of Health (K12 NS080223) and the Esther A. & Joseph Klingenstein Fund.

Competing interests

Parts of the technology described here are patent pending under 'Electroencephalography (EEG) Electrode Arrays and Related Methods of Use' U.S. Patent Application # PCT/US2020/051400. F. S. declares financial interest in Blackrock Microsystems LLC and Sentiomed, Inc., managed by University of Utah's COI management. W.K.D. and D.F. declare financial interest in Neuroview Technology overseen by NYU Grossman School of Medicine's COI management. D.F. also receives salary support for consulting and clinical trial related activities performed on behalf of The Epilepsy Study Consortium, a non-profit organization; receives no personal income for these activities. NYU receives a fixed amount from the Epilepsy Study Consortium towards Dr. Friedman's salary. Within the past two years, The Epilepsy Study Consortium received payments for research services performed by Dr. Friedman from Alterity, Baergic, Biogen, BioXcell, Cerevel, Cerebral, Jannsen, Lundbeck, Neurocrine, SK Life Science and Xenon. D.F. has also served as a paid consultant for Neurelis Pharmaceuticals and Receptor Life Sciences. O.D. has equity and/or compensation from Privateer Holdings, Tilray, Receptor Life Sciences, Qstate Biosciences, Tevard, Empatica, Engage, Egg Rock/Papa & Barkley, Rettco, SilverSpike and California Cannabis Enterprises. He has received consulting fees from GW Pharma, Cavion and Zogenix. S.R.S. has received salary/research support for clinical trials from Eisai, Monteris, Neuropace, UCB and Sunovion. Within the past two years, S.R.S. has received payments for consulting/advisory boards from Acquestive, Basilea, Blackthorn Therapeutics, LivaNova, Monteris, Neuropace, SK Lifesciences and UCB.

Supplementary material

Supplementary material is available at *Brain Communications* online.

References

1. Englot DJ, Chang EF. Rates and predictors of seizure freedom in resective epilepsy surgery: An update. *Neurosurg Rev*. 2014;37:389–405.
2. Chen Z, Brodie MJ, Liew D, Kwan P. Treatment outcomes in patients with newly diagnosed epilepsy treated with established and new antiepileptic drugs. *JAMA Neurol*. 2018;75:279.
3. Kwan P, Schachter SC, Brodie MJ. Drug-resistant epilepsy. *New Eng J Med*. 2011;365:919–926.
4. Englot DJ, Birk H, Chang EF. Seizure outcomes in nonresective epilepsy surgery: An update. *Neurosurg Rev*. 2017;40:181–194.
5. Landazuri P, Shih J, Leuthardt E, *et al*. A prospective multicenter study of laser ablation for drug resistant epilepsy – One year outcomes. *Epilepsy Res*. 2020;167:106473.
6. Ali R, Air EL. Surgical therapies for epilepsy. In: Spanaki MV and Wasade VS, eds. *Understanding epilepsy: A study guide for the boards*. Cambridge University Press; 2019:417–431.
7. Malmgren K, Edelvik A. Long-term outcomes of surgical treatment for epilepsy in adults with regard to seizures, antiepileptic drug treatment and employment. *Seizure* 2017;44:217–224.
8. Chang EF, Clark A, Smith JS, *et al*. Functional mapping–guided resection of low-grade gliomas in eloquent areas of the brain: Improvement of long-term survival. *J Neurosurg*. 2011;114:566–573.
9. Nair DR, Laxer KD, Weber PB, *et al*. Nine-year prospective efficacy and safety of brain-responsive neurostimulation for focal epilepsy. *Neurology*. 2020;95:e1244–e1256.
10. Gooneratne IK, Green AL, Dugan P, *et al*. Comparing neurostimulation technologies in refractory focal-onset epilepsy. *J Neurol Neurosurg Psychiatry*. 2016;87:1174–1182.
11. Franzini A, Moosa S, Servello D, *et al*. Ablative brain surgery: An overview. *Int J Hyperthermia*. 2019;36:64–80.
12. Rosenow F. Presurgical evaluation of epilepsy. *Brain* 2001;124:1683–1700.
13. NeuroPace. *RNS system physician manual*. NeuroPace, Inc; 2020.
14. Jehi L. The epileptogenic zone: Concept and definition. *Epilepsy Curr*. 2018;18:12–16.
15. Staba RJ, Stead M, Worrell GA. Electrophysiological biomarkers of epilepsy. *Neurotherapeutics* 2014;11:334–346.
16. Stead M, Bower M, Brinkmann BH, *et al*. Microseizures and the spatiotemporal scales of human partial epilepsy. *Brain* 2010;133:2789–2797.
17. Schevon CA, Goodman RR, McKhann G, Emerson RG. Propagation of epileptiform activity on a submillimeter scale. *J Clin Neurophysiol*. 2010;27:406–411.
18. Schevon CA, Tobochnik S, Eissa T, *et al*. Multiscale recordings reveal the dynamic spatial structure of human seizures. *Neurobiol Dis*. 2019;127:303–311.
19. Yang JC, Paulk AC, Salami P, *et al*. Microscale dynamics of electrophysiological markers of epilepsy. *Clin Neurophysiol*. 2021;132:2916–2931.
20. Buzsáki G, Anastassiou CA, Koch C. The origin of extracellular fields and currents—EEG, ECoG, LFP and spikes. *Nat Rev Neurosci*. 2012;13:407–420.
21. Stricsek G, Lang MJ, Wu C. Chapter 16 - stereoelectroencephalography (sEEG) versus grids and strips. In: Raslan AM and Burchiel KJ, eds. *Functional neurosurgery and neuromodulation*. Elsevier; 2019:113–120.
22. Schevon CA, Ng SK, Cappell J, *et al*. Microphysiology of epileptiform activity in human neocortex. *J Clin Neurophysiol*. 2008;25:321–330.
23. Chiang CH, Wang C, Barth K, *et al*. Flexible, high-resolution thin-film electrodes for human and animal neural research. *J Neural Eng*. 2021;18:045009.
24. Orsborn AL, Wang C, Chiang K, Maharbiz MM, Viventi J, Pesaran B. Semi-chronic chamber system for simultaneous subdural electrocorticography, local field potentials, and spike recordings. In 2015 7th International IEEE/EMBS Conference on Neural Engineering (NER); 2015.
25. Esteller R, Echauz J, Tcheng T, Litt B, Pless B. Line length: An efficient feature for seizure onset detection.
26. Pesaran B, Vinck M, Einevoll GT, *et al*. Investigating large-scale brain dynamics using field potential recordings: Analysis and interpretation. *Nat Neurosci*. 2018;21:903–919.
27. Stacey WC, Kellis S, Greger B, *et al*. Potential for unreliable interpretation of EEG recorded with microelectrodes. *Epilepsia* 2013;54:1391–1401.
28. Fernandez E, Greger B, House PA, *et al*. Acute human brain responses to intracortical microelectrode arrays: Challenges and future prospects. *Front Neuroeng*. 2014;7:24.
29. Chui J, Manninen P, Valiante T, Venkatraghavan L. The anesthetic considerations of intraoperative electrocorticography during epilepsy surgery. *Anesth Analg*. 2013;117:479–486.
30. Trumpis M, Chiang CH, Orsborn AL, *et al*. Sufficient sampling for kriging prediction of cortical potential in rat, monkey, and human microECoG. *J Neural Eng*. 2020.

31. Hill M, Rios E, Sudhakar SK, *et al*. Quantitative simulation of extracellular single unit recording from the surface of cortex. *J Neural Eng*. 2018;15:056007.
32. Wang Y, Goodfellow M, Taylor PN, Garry DJ, Baier G. Computational modelling of micro-seizures and focal seizure onset. In Paper presented at: Computational Nueorscience Meeting; BMC Neuroscience volume 14, Article number: P14 (2013) ; Paris, France.
33. Chiang C-H, Won SM, Orsborn AL, *et al*. Development of a neural interface for high-definition, long-term recording in rodents and nonhuman primates. *Sci Transl Med*. 2020;12:eaay4682.
34. Ray S, Maunsell JHR. Different origins of gamma rhythm and high-gamma activity in macaque visual cortex. *PLoS Biology*. 2011;9: e1000610.
35. Ray S, Crone NE, Niebur E, Franaszczuk PJ, Hsiao SS. Neural correlates of high-gamma oscillations (60-200 Hz) in macaque local field potentials and their potential implications in electrocorticography. *Journal of Neuroscience*. 2008;28:11526–11536.
36. Son AY, Biagioni MC, Kaminski D, Gurevich A, Stone B, Di Rocco A. Parkinson's disease and cryptogenic epilepsy. *Case Rep Neurolog Med*. 2016;2016:1–4.